Ceramics International

Effect of annealing treatments on the mechanical behaviour of UHTCMCs prepared by Mild Polymer Infiltration and Pyrolysis

--Manuscript Draft--

Manuscript Number:	CERI-D-22-10114
Article Type:	Full length article
Keywords:	A precursors: organic; C mechanical properties; D boride; E Structural applications
Corresponding Author:	Luca Zoli, Ph.D CNR-ISTEC Faenza, ITALY
First Author:	Francesca Servadei
Order of Authors:	Francesca Servadei
	Luca Zoli, Ph.D
	Pietro Galizia
	Cesare Melandri
	Simone Failla
	Diletta Sciti
Abstract:	C f /ZrB 2 -SiC composites were produced by slurry impregnation followed by six cycles of polymer infiltration and pyrolysis at 1000 °C. Despite the mild temperature of pyrolysis, the flexural strength of this composite showed values in excess of 500 MPa even at elevated temperature, up to 1400 °C. The abrupt decay of strength at 1500 °C stimulated the need to investigate the effect of additional thermal treatments enabling the crystallization of the amorphous polymer derived SiC(O). Annealing treatments, carried out between 1400 °C and 1900 °C, led to evident microstructural changes that in turn affected the flexural strength measured both at room temperature and at 1500 °C. The microstructural evolution was carefully analysed and 1400 °C was identified as the best trade-off between temperature of the annealing treatment and mechanical performance. After annealing at 1400 °C, the strength of the composite at room temperature decreased from the initial 500 MPa for untreated samples to 300 MPa due to the creation of new porosity, but this strength value was then maintained up to 87% at 1500 °C. Annealing at higher temperatures were detrimental for microstructure and strength.
Suggested Reviewers:	mattia biesuz, Ph.D Researcher, University of Trento Department of Industrial Engineering mattia.biesuz@unitn.it Researcher in material science with a focus on manufacturing and characterization of polymer derived ceramics
	Stefano Mungiguerra, Ph.D Researcher, University of Naples Federico II stefano.mungiguerra@unina.it Expert of characterization under extreme conditions for aerospace applications, He works on Ultra-high temperature Ceramics and Fiber reinfoced composites.
	Elisa Sani, Ph.D Researcher, National Institute of Optics National Research Council elisa.sani@ino.cnr.it She is an expert of characterization of materials for Energy applications such as Concentrating solar plant. She works on Ultra-high temperature Ceramics and UHTCMCs.
Opposed Reviewers:	

Dear General Editor Pietro. Vincenzini,

We are delighted of submitting our work “Effect of annealing treatments on the mechanical behaviour of UHTCMCs prepared by Mild Polymer Infiltration and Pyrolysis” to Journal of Alloys and Compounds.

As far as we know, the field of structural material designed for extreme hot environments (e.g. space applications and solar absorber), is well linked to the community of readers of this journal. The manuscript deals with the specific aspects of the science and technology of ceramic matrix composites for ultra-high temperature applications.

We designed and manufactured under mild temperature an innovative uncoated pitch-based carbon fibre reinforced polymer derived ceramic matrix composite materials containing a large fraction of an Ultra-High Temperature Ceramic phases. Because manufacturing of ceramic matrix composite is and energy-intensive process, our challenge was to find the best trade-off to balance performance and cost effectiveness of structural materials designed for very specific hot topic applications.

We methodically investigated the correlation of microstructure with thermo-mechanical properties of material, after heat treatments from 1100 °C to 1900 °C, supplying a guideline to our community working on in this topic for design and manufacturing stable materials.

We believe the manuscript deals with the criteria of the Journal.

Best regards

Luca Zoli, Ph.D

Structural and Functional Ceramics

CNR – ISTEC: National research council - Institute of Science and Technology for Ceramics

Via Granarolo, 64 I-48018 FAENZA (RA) - ITALY

Tel. +39 0546 699723

www.istec.cnr.it

Effect of annealing treatments on the mechanical behaviour of UHTCMCs prepared by Mild Polymer Infiltration and Pyrolysis

Francesca Servadei, Luca Zoli*, Pietro Galizia, Cesare Melandri, Simone Failla, Diletta Sciti

CNR-ISTEC, Institute of Science and Technology for Ceramics, Via Granarolo 64, I-48018 Faenza, Italy

**Author to whom correspondence should be addressed: Luca Zoli, luca.zoli@istec.cnr.it*

Abstract

C_f/ZrB_2-SiC composites were produced by slurry impregnation followed by six cycles of polymer infiltration and pyrolysis at 1000 °C. Despite the mild temperature of pyrolysis, the flexural strength of this composite showed values in excess of 500 MPa even at elevated temperature, up to 1400 °C. The abrupt decay of strength at 1500 °C stimulated the need to investigate the effect of additional thermal treatments enabling the crystallization of the amorphous polymer derived SiC(O). Annealing treatments, carried out between 1400 °C and 1900 °C, led to evident microstructural changes that in turn affected the flexural strength measured both at room temperature and at 1500 °C. The microstructural evolution was carefully analysed and 1400 °C was identified as the best trade-off between temperature of the annealing treatment and mechanical performance. After annealing at 1400 °C, the strength of the composite at room temperature decreased from the initial 500 MPa for untreated samples to 300 MPa due to the creation of new porosity, but this strength value was then maintained up to 87% at

1500 °C. Annealing at higher temperatures were detrimental for microstructure and strength.

Keywords: A Precursors: organic; C Mechanical properties; D Boride; E Structural applications;

Introduction

Structural and functional components made of carbon and ceramic matrix composites (CMCs) have been identified as sustainable solutions, which reduce total costs and environmental impact for aerospace (e.g. heat shield, leading edges, rocket nozzles), automotive (e.g. brake disc and pad), heat treating (fan, piston, mould, trays..etc), concentrating solar power systems (receiver), and semiconductors fields. Such materials have excellent thermo-mechanical properties, lightness and low deformability [1,2]. Based on the application, porous or dense materials are designed, however, those materials are still limited to specific applications because they are very expensive compared to other structural materials [3]. Indeed, despite carbon/carbon (C/C) composites can withstand extremely hot environments (up to 3000 °C) under not-oxidizing atmosphere (e.g. rocket nozzle and nose cone space vehicles, brake disc of supercars), several months are required to manufacture components and they are plagued by severe erosion after just a single mission or race [4]. On the other hand, silicon carbide-based composites (C/C-SiC [5], C/SiC [6], and SiC/SiC [7]) are reusable components (e.g. heat shields, turbine blades, brake disc, solar receiver) because they form a SiO_2 glass layer that is an excellent oxygen barrier; however, their application is limited to temperature below 1600 °C [3]. By introducing in the matrix Ultra-High Temperature Ceramics (UHTCs) [8][9][10], a class of materials characterised by

extremely high melting points (~3000 °C) that showed high stability in harsh environments, it is possible to overcome the limits of the current CMCs and also improve self-healing capability [11]. Especially, when zirconium diboride or hafnium diboride were combined with SiC or silicides the oxidation resistance was improved over 2000 °C due to the formation of compact scale with a complex Me-Si-B-O microstructure with low vapour pressure [12]. Moreover, multiphase bulk UHTCs and UHTCMCs find other applications such as porous burners and solar absorbers [13][14].

In a previous work [15], we presented a novel two-step process (water-based slurry impregnation plus mild PIP at 1000 °C) to manufacture C_f/ZrB_2-SiC composites to keep the cost of the process as low as possible, exploiting the benefit to combine: uncoated pitch-based carbon fibre (Cf), with a large fraction of ZrB_2 (21–30 vol%) and amorphous polymer derived SiC. The water-based impregnation allowed an excellent dispersion of ZrB_2 particles around each fibre thus overcoming typical nonuniform matrix microstructure as the result of polymer-based slurries [16], and was less impacting on the environment thanks to use of water-based slurries. The obtained composites showed fast passivation up to 1650 °C, excellent mechanical properties and defect tolerance, with a flexural strength of 200 MPa with 2D preforms and 500 MPa with unidirectional preforms, in agreement with the literature on this topic [17][18].

In this work, we first investigated the elevated temperature strength from 1000 °C to 1500 °C of unidirectional uncoated pitch-based C_f/ZrB_2-amorphous SiC composite to push the material towards its operational limit. Then, we studied the effect of just one single annealing treatment on the SiC(O) crystallization and how this affected room and elevated temperature (1500°C) flexural strength. Heat treatments were conducted at every 100 °C in the temperature range 1100 °C – 1900 °C. In the literature, the best

pyrolysis temperature is still matter of debate, ranging between 900 °C and 1600 °C. Li et al. [18] fabricated C/ZrC-SiC and C/ZrB_2-ZrC-SiC by subsequent cycles of impregnation and pyrolysis at 900 °C associated with heating at 1500 °C to increase the crystallinity. The team of Y. Blum [19] reported the development of some UHTC coatings using slurries of ZrB_2 and SMP-10 followed by heat treatment up to 1500 °C. Uhlmann et al. [20] prepared PAN-based C_f/SiC-ZrB_2-TaC composites exhibiting an excellent thermo-chemical resistance by adding ZrB_2 and Ta powder within the pre-ceramic slurry of C/SiC, followed by thermal treatments at 1600 °C.

Available papers hardly report the flexural strength at elevated temperature. One of the few examples is the work of Hu et al. [16], who fabricated PAN-based C/SiC-ZrB_2 composites with 10–25 vol% ZrB_2 by infiltration using a ZrB_2 powder/polycarbosilane-based slurry and pyrolysis at 1200 °C (not reported the reason), achieving a flexural strength of 367 MPa at room temperature and strength retention of 74% at 1800 °C (32% at 2000 °C).

In this perspective, this work reported a methodical study that explored a large range of temperatures and analysed the step-by step microstructural evolution with special emphasis on reaction phenomena observed at ZrB2/SiC(O) interface and fibre/matrix interface.

1. Materials and methods

Commercially available products were used for the preparation of polymer-derived C_f/ZrB_2-SiC composites, fibres: unidirectional (UD) ultra-high modulus pitch-based carbon fibre fabrics (Granoc, Japan; fabric: UF-XN80-300, areal weight 330 g/m^2; yarn: XN80-60S, diameter 10 μm, density 2.17 g/cm^3, tensile modulus 780 GPa, tensile

strength 3.4 GPa); ceramic powders: α-SiC (Grade UF-25, H.C. Starck, Germany; specific surface area 23–26 m^2/g, D50 0.45 μm, impurities (wt.%): 2.5 O), and ZrB_2 (Grade B, H.C. Starck, Germany; specific surface area 1.0 m^2/g, particle size range 0.5–6 μm, impurities (wt.%): 2 O, 0.25 C, 0.25 N, 0.2 Hf, 0.1 Fe); polymeric precursor of SiC: allylhydrido polycarbosilane (StarPCS™ SMP-10, Starfire System Inc., U.S.A.; density 0.998 g/cm^3, viscosity 40–100 cPs at 25°C), and cross-linker catalyst: trimethyl(methylcyclopentadienyl) platinum(IV), $MePtCpMe_3$ (Sigma Aldrich; purity 98%).

The reference sample (labelled as 6PIP-10) was manufactured by slurry impregnation of UD carbon fibre preforms with aqueous ZrB_2-10 vol% SiC powder suspension and stacking them in a 0/0° configuration, followed by six cycles of polymer infiltration with SMP-10 and pyrolysis at 1000°C under argon flow. Further details of experimental procedures are reported in our previous work [15].

Bars with dimensions 25 mm × 2.5 mm × 2 mm and 10 mm × 10 mm × 2 mm sized coupons were machined from the reference sample. Then, nine batches of 4 samples were heat treated at every 100 °C in the range 1100°C–1900°C in a resistance-heated graphite furnace (1000-3060-FP12, Astro Industries Inc., U.S.A.) under a flowing Ar atmosphere (ramp 600°C/h up to target temperature and dwell for 2h, free cooling in Ar). Each batch was labelled as A-X, where X is a number from 11 to 19. After each heat treatment, bulk densities were determined via weight-to-geometric volume ratio (balance accuracy ±0.01 mg), mass changes were calculated as weight loss divided by starting weight, while volume changes were calculated as the ratio of volume difference before and after annealing to the initial volume. Mercury intrusion porosimetry (MIP) was carried out to determine bulk densities, skeletal densities (where measured volume

excludes open porosity) and open porosity in the range 0.0058−100 μm (Pascal 140 and Pascal 240 series, Thermo Finnigan, U.S.A.).

Crystalline phases were detected by X-ray diffraction (XRD) collecting patterns from 10 to 80° (step 0.02°, step time 0.5 s) on coupon surfaces using a diffractometer with CuKα radiation (D8 Advance, Bruker, Germany).

Microstructural features and elemental composition of the as-obtained material and annealed specimens were analysed using field emission gun-scanning electron microscope (FE-SEM, ZEISS Sigma, Carl Zeiss Microscopy GmbH, Germany) and energy dispersive X-ray spectroscopy (EDS, INCA Energy 300, Oxford instruments, UK) on polished sections. 4-point flexural strength of reference and annealed samples were measured in a screw-driven load frame (Z050, Zwick-Roell, Germany) with a lower span of 20 mm and an upper span of 10 mm, cross-head rate of 1 mm/min, on bars 25.0 mm × 2.5 mm × 2.0 mm (length by width by thickness, respectively), following the guidelines of EN 843-1:2006. Tests in the range 1000°C–1500°C were carried out under Ar flow (3.5 L/min) to limit oxidation effect. Fracture surfaces were studied using a digital microscope (RH-2000, Hirox Europe, France) and FE-SEM/EDS.

2. Results and discussion

2.1. Features of as-obtained material

The reference sample (6PIP-10) contained around 30 vol% carbon fibres, 64% vol% matrix (ZrB_2-SiC_p-$SiC(O)_{PDC}$), 6% porosity [15], see Table 1 and Fig.1a-e. $SiC(O)_{PDC}$ (grey contrast) was hardly distinguishable from SiC_p particles due to the low contrast difference (Fig. 1a,b). In general, SiC_p was mainly found homogeneously mixed with ZrB_2 particles and distributed around the fibres, whereas $SiC(O)_{PDC}$ was found either finely dispersed in the ZrB_2 matrix or in large spots filling the cavities and

in thin films surrounding the fibres (Fig. 1c). Fig. 1d highlights unreacted ZrB_2 grain boundary with the amorphous $SiC(O)_{PDC}$, see EDS signal Si-C-O in Fig. 1e. Kaur [21] found that SMP-10 treated at 1100 °C has the following empirical formula: $SiC_{1.19}O_{0.16}$, exhibiting 7.2 wt% segregated carbon and more than 10 wt% silica.

Table 1. Resulting composition (volumetric amounts of carbon fibres (C_f), zirconium diboride (ZrB_2), powder-derived silicon carbide (SiC_p) and polymer-derived silicon carbide (SiC_{PDC})) and open porosity of the reference sample obtained by 6 PIP cycles at 1000°C.

Sample	**C_f (vol%)**	**ZrB_2 (vol%)**	**SiC_p (vol%)**	**$SiC(O)_{PDC}$ (vol%)**	**Porosity (%)**
6PIP-10	30	29	3	32	6

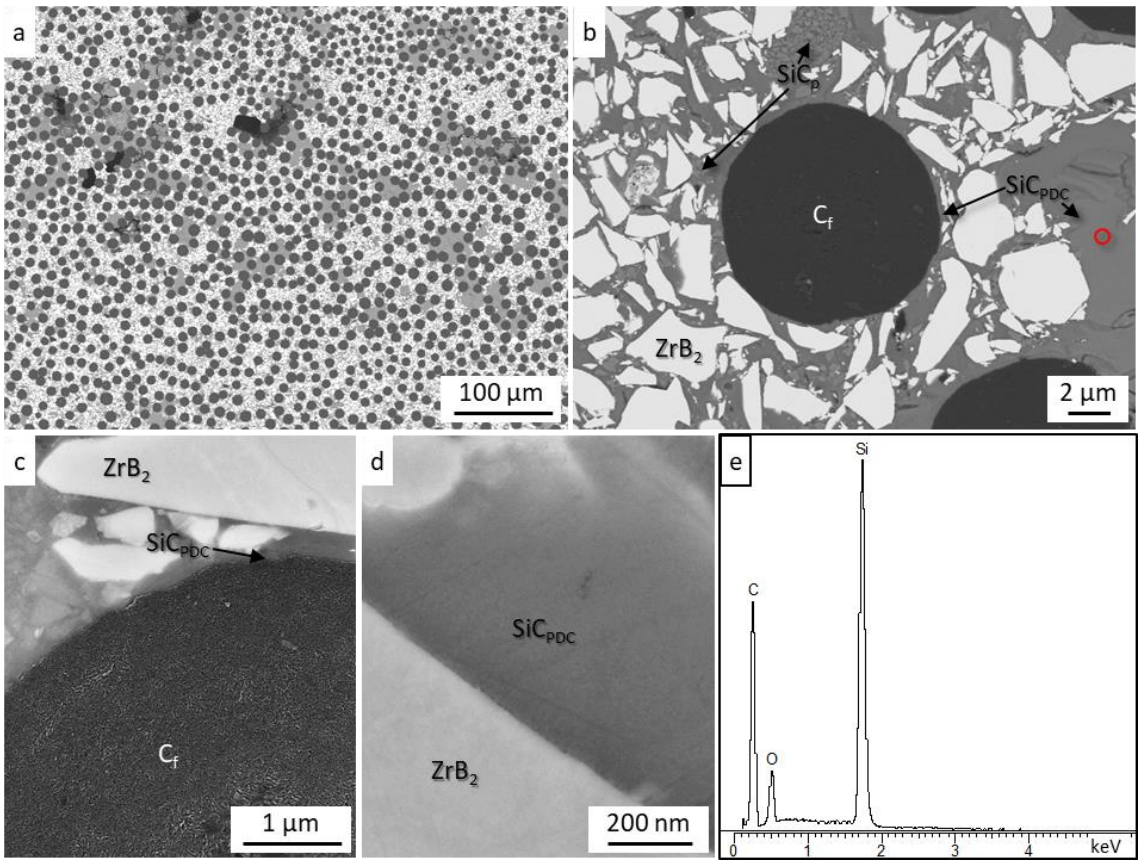

Fig. 1. Polished section of C_f/ZrB_2-SiC obtained by 6 PIP cycles at 1000°C (sample 6PIP-10). (a) Low magnification micrograph; C_f is the dark phase, ZrB_2 is the bright phase, SiC is the grey phase, while black areas are pores. (b) A single fibre surrounded by ZrB_2-SiC_p-SiC_{PDC} matrix. Detail of (c) fibre/matrix interface and (d) ZrB_2 grain boundaries embedded in amorphous PDC. (e) EDS spectrum (EDS spot is marked in (b)) of SiC_{PDC} resulted in SiC(O).

In Fig. 2, the values of flexural strength of reference sample 6PIP-10 from room temperature to 1500 °C and examples of load-displacement curves obtained through 4-point bending tests at room and elevated temperature are reported.

6PIP-10 retained an excellent flexural strength (even higher than at room temperature) at any temperature tested up to 1400 °C (Fig. 2a). Load-displacement curves related to the tests at room temperature (Fig. 2b) and tests at 1300 °C (Fig. 2c) showed that failure likely occurred with the same mechanism. At 1400 °C, the curve revealed a more graceful fracture. At 1500 °C, no value could be recorded due to plastic deformation of the specimen, very likely induced by softening of amorphous SiC(O) and other phenomena as explained later. Optical image of the bar tested at 1500°C and details of the microstructure are reported in the supplementary material, Fig. S1.

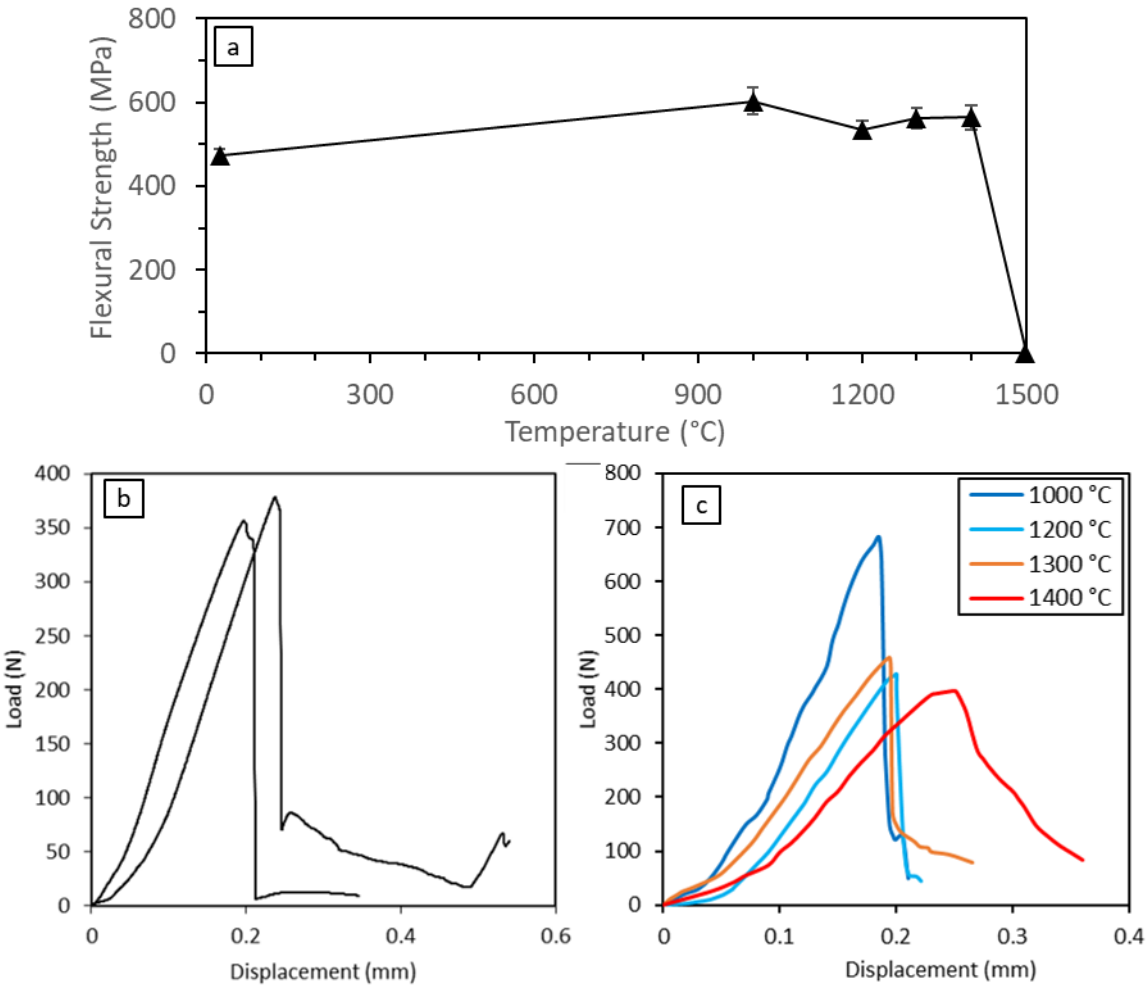

Fig. 2.a) Plot showing the flexural strength for reference sample 6PIP-10 from RT to 1500 °C (under argon flow). b) An example of load-displacement curves obtained through 4-point bending tests at room and c) elevated temperature (under Ar flow).

2.2. Features of annealed materials

Bulk and skeletal densities, open porosities, weight loss and volume variations measured after annealing at temperature from 1100 °C to 1900 °C are represented in the plot in Fig. 3 (values are reported in support information Table S1). All these parameters were stable up to 1400 °C, abruptly changed at 1500 °C and 1600 °C, and then reached a plateau between 1700 °C and 1900 °C. In particular, in the range 1400 °C–1600 °C, weight losses increased from 0.4 to 10% and residual porosity jumped from 6% to 20% (1500 °C) and at about 30% at 1600 °C.

Weight loss occurred because of crystallization of β-SiC via carbothermal reaction between the Si-O bonds and excess carbon of the silicon oxycarbide [22]. This also explains the increase in the skeletal density. Indeed, density of SMP-10 is about 2.5 g/cm^3 when it is pyrolysed at 1000 °C and increases to 3.1 g/cm^3 after treatment at 1600 °C [23]. In agreement with Kumar et al. [1,2], the following reactions (1–4) well describe the typical conversion of amorphous polymer-derived SiC into β-SiC and justify the loss of weight found after heat treatments:

$$SiC + SiO_2 \rightarrow 2\ SiO(g) + C \quad (1)$$

$$SiO_2 + 3\ C \rightarrow SiC + 2\ CO(g) \quad (2)$$

$$SiO(g) + 2\ C \rightarrow SiC + 2\ CO(g) \quad (3)$$

$$SiO(g) + CO \rightarrow SiC + CO_2(g) \quad (4)$$

The overall reaction (5) is reported below

$$SiC_xO_y \rightarrow SiC + 1\text{-}(x+y)\ SiO(g) + x\ CO(g) \quad (5)$$

According to the observed weight loss, the recombination of SiO(g) with C or CO(g), reactions (3–4), is hindered by gas removal during heat treatment (flux of argon).

The low weight loss until 1400 °C was in agreement with TGA studies on SMP-10 reported in ref. [19][22]. In the range 1400 °C–1600 °C Yin et al. [24], who prepared CMCs using a different type of polycarbosilane, reported a strong mass loss amounting to 17%, similar to the present case after normalization. As demonstrated by Kaur et al. [22], heat treatments at high temperature (i.e. 1700 °C) lead to stoichiometric SiC composition, but at the same time the release of oxygen and excess carbon in form of CO causes mass loss and an increment of porosity. Furthermore, Kaur et al. [22] reported that as the temperature goes up an increasingly shrinkage occurred in bulk ceramics.

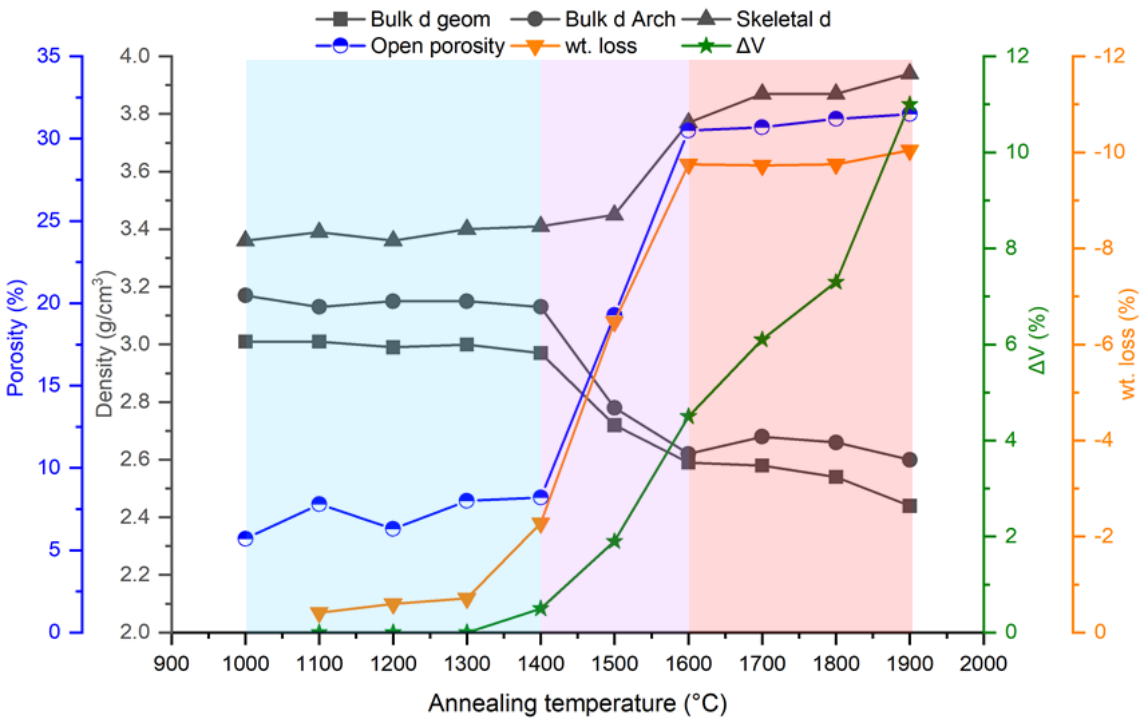

Fig. 3. Plot representing bulk densities measured via geometric method and via MIP, skeletal density, open porosity, weight loss and volume variation as a function of the annealing temperature.

XRD patterns on reference sample and annealed samples (Fig. 4) confirmed substantial changes in the crystallinity of species starting from 1400 °C. SiC(O) obtained as product of pyrolysis of the polycarbosilane at temperature below 1300 °C resulted amorphous and generated only poorly defined humps in the X-ray scattering profiles. Broad diffractions peaks at 2θ = 36°, 60° and 72° corresponding to β-SiC polymorph (PDF #65-0360) started to appear at 1400 °C and became sharper by increasing the temperature, confirming the occurrence of SiC(O) conversion to nano-sized SiC crystals. From A-16 to A-19 a gradual increase of β-SiC conversion with grown crystallites up to 44 nm was observed, in agreement with [25], moreover XRD patterns revealed the presence of peaks at 2θ = 34° and 60° which are attributable to α-SiC polymorph (PDF #49-1428).

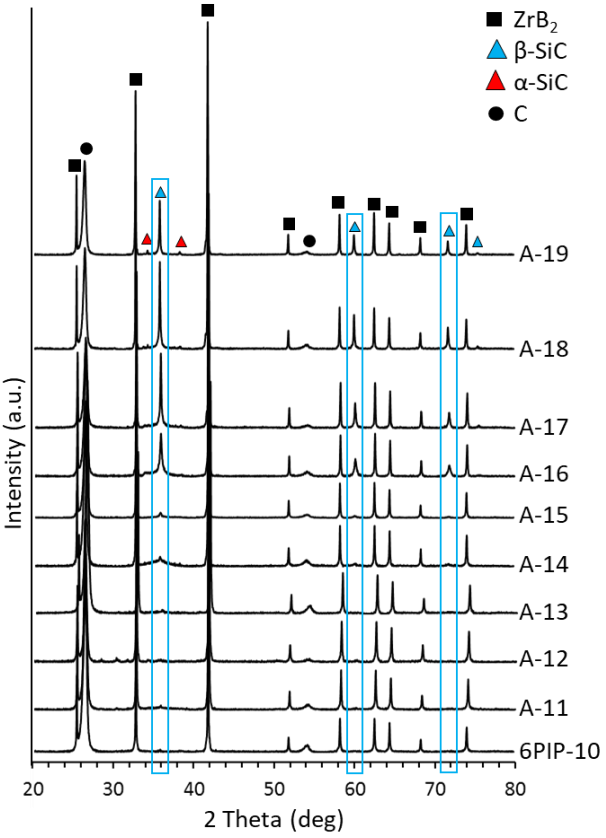

Fig. 4. X-ray diffraction patterns collected on the surface of the reference sample 6PIP-10 and samples annealed at temperature from 1100 °C to 1900 °C.

The cross sections of annealed samples up to 1300 °C (A-11 – A-13) confirmed morphologies similar to sample 6PIP-10 (see Fig. 1). According to XRD patterns, minimal microstructural changes appeared at 1400 °C (Fig. 5, A-14). Indeed, occurrence of thin cracks in larger pockets of SiC(O) was observed due to its crystallization. Notably, surficial oxidation of ZrB_2 grains occurred with formation of tiny zirconia particles (see details in Fig. 5, A-14 and A-15 middle), with the consequent transformation of the sharp edges of the ZrB_2 particles to blunt. This phenomena was also detected by Blum et al. [19] and it could be explained through the reaction (6):

$$ZrB_2 + 5\ SiO_2 \rightarrow ZrO_2 + 5\ SiO(g) + B_2O_3(g) \qquad (6)$$

The thermodynamics of the reaction was calculated by HSC 6.0 and FactSage web [26] software in the range 1000 °C – 2500 °C and from 1 mbar to 1 bar, see isobaric multiphase equilibria graph in supplementary material, Fig. S2. The reaction, unfavourable up to 1900°C at 1 bar, becomes favourable from 1500 °C at 1 mbar (e.g. inside the specimen).

At 1600 °C, the matrix appeared visibly porous. In particular, the larger pockets of PDC appeared as porous/sponge-like plates (Fig. 5, A-16 middle and right). Furthermore, reactions (1–2) between Si/SiO_x species (PDC) and C (fibres) occurred, despite the fibre/matrix interface was still smooth (Fig. 5, A-16 right). Tiny SiC particles were found along the fibre profile, probably due to carbothermal reduction of SiO_x phases in the proximity of the fibre surface, see reaction 2 and reaction 3.

Between 1700 °C and 1900 °C, ZrB_2 grains passed from an acicular to a more rounded shape and formed a stronger bond to the converted SiC phase. Moreover, small zirconia particles disappeared and ZrB_2 particles were visible in their place due to reaction (7):

$$ZrO_2 + B_2O_3 + 5C \rightarrow ZrB_2 + 5CO \qquad (7)$$

Finally, the fibre profile became increasingly jagged due to reactions of oxide phases with carbon fibre surface.

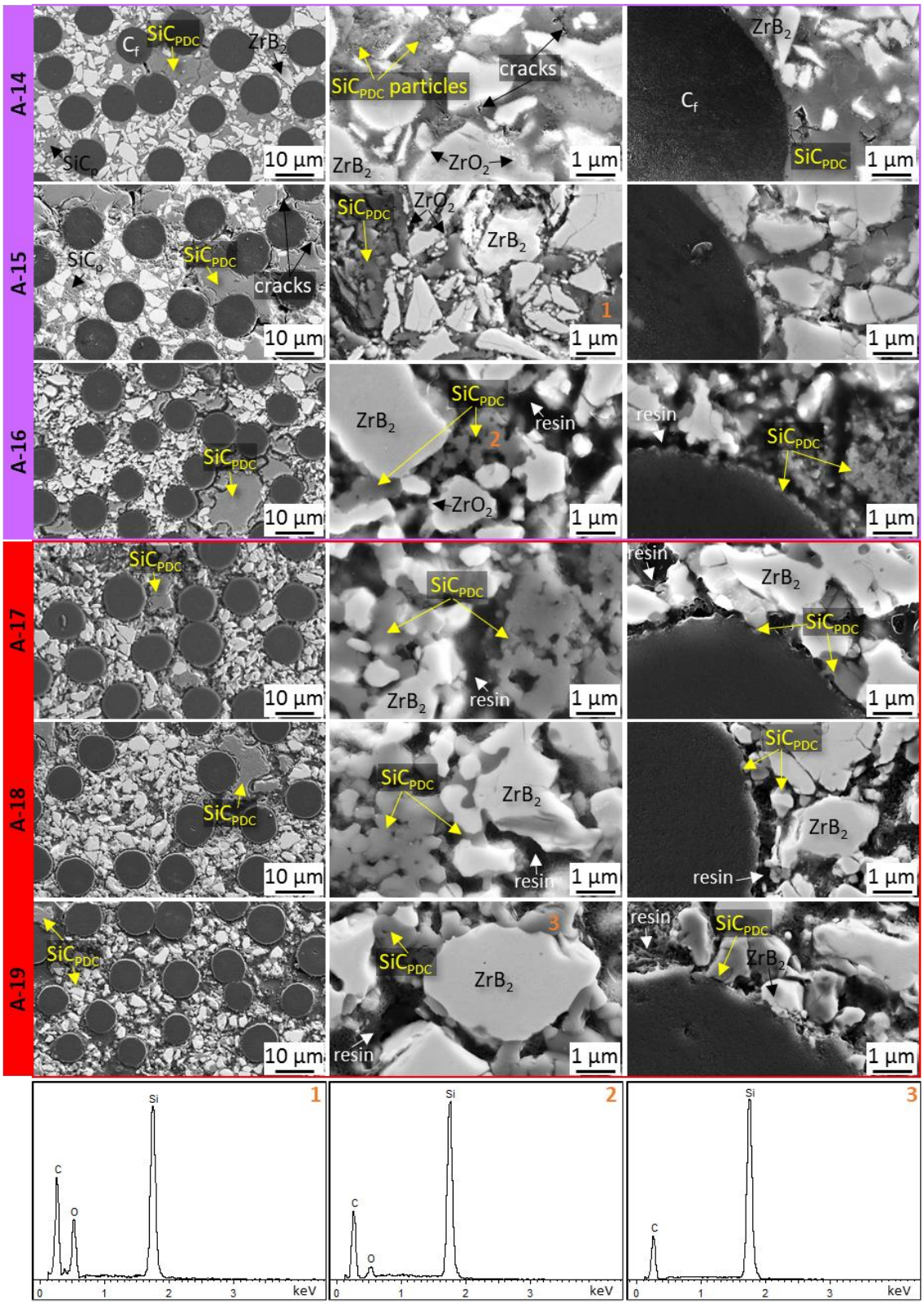

Fig. 5. Polished cross section of samples annealed at 1400 °C –1900 °C, showing for each sample: intra-bundle region (left), a detail of the matrix highlighting the different morphologies of SiC_{PDC} (middle), a detail of the fibre/matrix interface (right). At the bottom, EDS spectra of the polymer-derived SiC(O) and SiC as numbered.

RT bending tests on annealed samples: Room temperature values are summarized in Table 2 for samples annealed in the range 1400 °C – 1900 °C, while load-displacement curves are reported in Fig. 6a,b.

Table 2. Flexural strength by 4-point bending test of reference sample 6PIP-10 and selected annealed samples (A-xx) tested at room temperature and at 1500 °C (under argon flow).

Sample	σ 4-pt RT (MPa)	σ 4-pt 1500 °C (MPa)
6PIP-10	474 ± 14	invalid
A-14	300 ± 6	262 ± 34
A-15	173 ± 21	62 ± 9
A-16	184 ± 23	92 ± 1
A-17	200 ± 6	168 ± 54
A-18	161 ± 6	105 ± 45
A-19	213 ± 8	100 ± 85

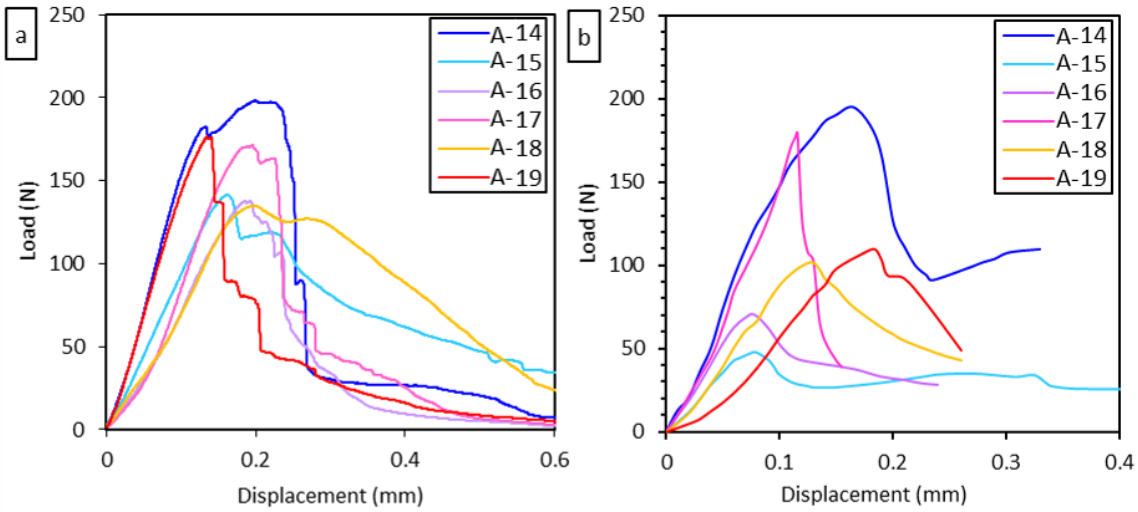

Fig. 6. An example of load-displacement curves of annealed samples obtained through 4-point bending tests at room and c) elevated temperature (under Ar flow).

After annealing, room temperature bending strength lose 36% and 55% – 63% for specimens A-14 and A-15 – A-19 samples, respectively [27,28]. No appreciable variation in the strength was noticed amongst A-15 – A-19 samples, despite the different pyrolysis conditions and levels of matrix porosity (i.e. 19–32%). This is mirrored in works of Kimura et al. [29–31], who realized C/C composites with the same

carbon fibre fraction but increasing level of porosity (manufactured by CVI). The authors demonstrated that a threshold of ~15% of porosity affects dramatically the strength of the C/C as it lowers the effective volume fraction of fibres on the stress–strain response.

The jagged stress-strain curves in the failure stage revealed a non-brittle behaviour of all the specimens, due to a pseudo-plasticity failure promoted from the weak fibre/matrix interface and the high porous weak matrix, in agreement with literature [32]. In fact, the annealing treatments affected the fibre/matrix interface leading to increasingly detached interfaces (Fig. 7) due to enhanced SiC crystallization. Failure occurred by multiple microcrackings, that proceeded highlighting phenomena of crack arresting, deflection or fibre bridging until total failure of the composite took place, as demonstrated by zig-zag load-displacement curves (Fig. 6b) and tortuous cracks paths (Fig. 7 left).

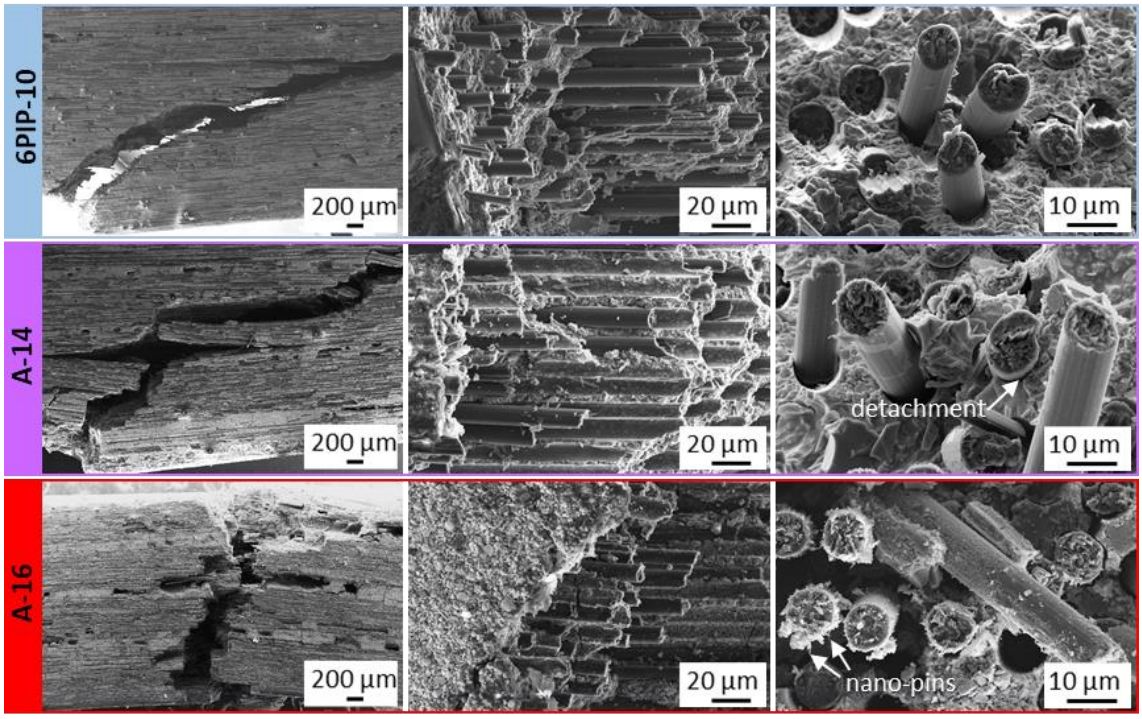

Fig. 7. Micrographs of bars of reference sample 6PIP-10 and samples annealed at 1400 °C (A-14) and 1600 °C (A-16) fractured by 4-pt bending test at room temperature, highlighting for each sample: lateral view showing crack path, tensile surface, fracture surface.

1500 °C bending tests on annealed samples: Differently from sample 6PIP-10, valid bending tests at 1500 °C were obtained for all annealed composites (see load-displacement curves in Fig. 6b), which showed quite scattered values and an average value from 62 MPa to 212 MPa (Table 2).

Bars of A-14, A-15 and A-16 batches plastically deformed during bending moment and large cracks opened in correspondence of point load application (see optical pictures of some tested bars in supplementary material, Fig. S3). Bar surfaces were covered by a dark silica glassy layer with a good adhesion to the bulk, only where the bar is bent it showed the tendency to spell-off baring undamaged C fibres. The failures were likely caused by a combination of bending and plastic deformation. In contrast, A-17 – A-19 samples appeared outwardly oxidized with a limited amount of glassy phases softening and no notable signs of plastic deformation (supplementary material, Fig. S3). A-17 gave the higher strength at 1500 °C among them.

3.3 Discussion: trade-off analysis to balance performance and post-annealing cost effectiveness

A strongly recommended functionality for materials to be used in extreme hot environments is thermal stability because it hinders the collapse of material at elevated temperature (1500 °C in this case). For polymer-derived ceramics like SiC(O) [33], thermal stability is intended to be the crystallization resistance of these ceramics with increasing of temperature (e.g 1350 °C). The loss of thermal stability and performance at elevated temperature are triggered by crystallization of SiC(O), which results in phase separation (SiO_2 and C), weight loss ($SiO_{(g)}$ and $CO_{(g)}$) and increase of porosity. In the bulk, the failure at elevated temperature is caused by formation of spurious phases at grain boundaries.

Much more recently, excellent thermal stability has been invoked for much more complex systems such as fibre-reinforced polymer-derived ceramics. For fibre-reinforced ZrB_2-SiC(O), in order to be operated in hot and harsh aerospace environments, the loss of performance at temperature beyond the crystallization threshold of SiC(O) seems to be mitigated by the cooperation among carbon fibres, SiC(O) and ZrB_2 matrix. Indeed, the resulting increment of porosity of the SiC(O) matrix is balanced by the presence of ZrB_2 fillers and the formation of a strong fibre/matrix interphase caused by reaction of C with oxides phases at grain boundaries, converting such spurious phases into stable UHTCs around carbon fibres.

-*Applications <1500 °C*: Reference material 6PIP-10 exhibited stable microstructure, excellent mechanical properties and a relatively low cost of production due to the mild PIP conditions used.

-*Applications ≥1500 °C*: In the plot in Fig. 8, the obtained values of open porosity, bulk density, RT and HT flexural strengths, and HT/RT flexural strengths ratio (with mean absolute error (MAE) as a shaded grey area) are reported for each sample. Sample 6PIP-10 is no longer suitable for this temperature range, while A-15 showed the worst high temperature flexural strength values. A-14 showed the best RT and HT strength among annealed samples and the highest HT/RT σ ratio (0.87). A-17 showed a 0.84 HT/RT strength ratio, but the notable amount of porosity (~30%) caused a notable loss of strength (~200 MPa) compared to the pristine untreated sample (~500 MPa).

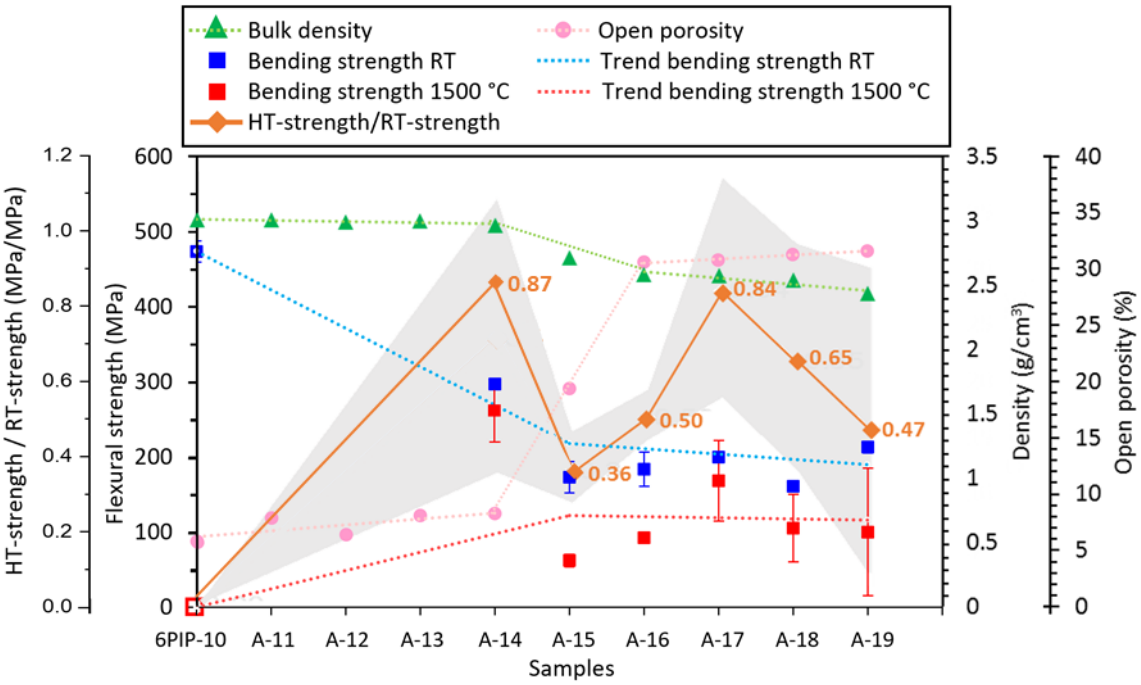

Fig. 8. Plot showing the bulk density and open porosity of reference sample 6PIP-10 and all annealed samples (at 1100 °C–1900 °C), RT and 1500 °C flexural strength, and HT-strength/RT-strength ratio for sample 6PIP-10 and samples annealed at 1400 °C–1900 °C (with MAE as a shaded grey area).

Within the samples developed in the present work, the composite A-14 seems to display the better chance to be selected as passive reusable heat shield of future space vehicles for Earth re-entry as it is (without Environmental barrier coating) while A-17 could be applied as structural porous layer (e.g sandwich panel, insulator) for aerospace, industrial or solar receiver in CSP.

4. Conclusions

The purpose of this work was to deduce the effect of annealing heat treatments of 2h (1100 °C to 1900 °C) on the microstructure and thermo-mechanical properties of unidirectional C_f/ZrB_2-SiC composite to help readers to design and manufacture the next generation materials for aerospace and high temperature solar absorbers in Concentrating Solar Power systems. A reference material was fabricated through a cycle of powder slurry impregnation followed by six repetitive PIP cycles at 1000 °C using a commercial allylhydrido polycarbosilane precursor (SMP-10), which are very mild

conditions for manufacturing UHTCMCs. Reference sample exhibited an amorphous SiC(O) matrix with porosity below 10% and a flexural strength over 550 MPa up to 1400 °C. Post pyrolysis heat treatments up to 1400 °C did not significantly affected the porosity neither the morphology of SiC(O), while annealing at temperature of 1500 °C and beyond led to conversion of amorphous SiC(O) into crystalline β-SiC and consequently to an increase of open porosity up to 30%. Flexural strength of annealed composites above 1500 °C resulted in performance deterioration at room temperature, reaching values not higher than of 215 MPa. Bending tests at 1500 °C revealed an improvement of the strength compared to material consolidated at mild conditions. Annealing at 1400 °C was identified as the best trade-off to balance performance and cost effectiveness to achieve dense materials with excellent performance up to 1500 °C. Annealing at 1700 °C was identified as the minimal heat treatment to complete crystallization of polymer derived SiC as well as the removal of oxide impurities on ZrB_2 and SiC grains to achieve a porous thermally stable composite.

CRediT authorship contribution statement

F. Servadei: Investigation, Data curation, Writing - original draft; L. Zoli: Conceptualization, Supervision, Methodology, Writing - review & editing. P. Galizia: investigation, Data curation, writing - review & editing; C. Melandri: investigation; D. S. Failla: heat treatment methodology, Sciti: Project administration, Funding acquisition, Writing - review & editing.

Declaration of competing interest

The authors declare that they have no known competing financial interests or personal relationships that could have appeared to influence the work reported in this paper.

Acknowledgements

The authors wish to thank A. Piancastelli for mercury intrusion porosimetry analysis and C. Capiani for X-ray diffraction analysis.

This work was supported by the European Union's Horizon 2020 "Research and innovation programme" [grant agreement N° 685594 (C^3HARME: Next Generation Ceramic Composites for Harsh Combustion Environment and Space)].

References

[1] S. Kumar, M.K. Misra, S. Mondal, R.K. Gupta, R. Mishra, A. Ranjan, A.K. Saxena, Polycarbosilane based UD C/SiC composites: Effect of in-situ grown SiC nano-pins on mechanical properties, Ceram. Int. 41 (2015) 12849–12860. doi:10.1016/J.CERAMINT.2015.06.122.

[2] P. Galizia, D. Sciti, N. Jain, Insight into microstructure and flexural strength of ultra-high temperature ceramics enriched SICARBON™ composite, Mater. Des. 208 (2021) 109888. doi:10.1016/j.matdes.2021.109888.

[3] N.P. Padture, Advanced structural ceramics in aerospace propulsion, Nat. Mater. 15 (2016) 804–809. doi:10.1038/nmat4687.

[4] W. Krenkel, Ceramic Matrix Composites: Fiber Reinforced Ceramics and their Applications, Wiley-VCH, Weinheim, 2008. doi:10.1002/9783527622412.

[5] W. Krenkel, F. Berndt, C/C-SiC composites for space applications and advanced friction systems, Mater. Sci. Eng. A. (2005). doi:10.1016/j.msea.2005.08.204.

[6] L. Zoli, D. Sciti, L.A. Liew, K. Terauds, S. Azarnoush, R. Raj, Additive Manufacturing of Ceramics Enabled by Flash Pyrolysis of Polymer Precursors with Nanoscale Layers, J. Am. Ceram. Soc. 99 (2016) 57–63. doi:10.1111/jace.13946.

[7] S. Azarnoush, F. Laubscher, L. Zoli, R. Raj, Additive Manufacturing of SiCN Ceramic Matrix for SiC Fiber Composites by Flash Pyrolysis of Nanoscale Polymer Films, J. Am. Ceram. Soc. 99 (2016) 1855–1858. doi:10.1111/jace.14145.

[8] D. Sciti, L. Zoli, T. Reimer, A. Vinci, P. Galizia, A systematic approach for horizontal and vertical scale up of sintered Ultra-High Temperature Ceramic Matrix Composites for aerospace – Advances and perspectives, Compos. Part B Eng. 234 (2022) 109709. doi:10.1016/j.compositesb.2022.109709.

[9] D. Sciti, P. Galizia, T. Reimer, A. Schoberth, C.F. Gutiérrez-Gonzalez, L. Silvestroni, A. Vinci, L. Zoli, Properties of large scale ultra-high temperature ceramic matrix composites made by filament winding and spark plasma sintering, Compos. Part B Eng. 216 (2021) 108839. doi:10.1016/j.compositesb.2021.108839.

[10] Y. Arai, R. Inoue, K. Goto, Y. Kogo, Carbon fiber reinforced ultra-high temperature ceramic matrix composites: A review, Ceram. Int. 45 (2019) 14481–14489.

[11] F. Servadei, L. Zoli, A. Vinci, P. Galizia, D. Sciti, Significant improvement of the self-protection capability of ultra-high temperature ceramic matrix composites, Corros. Sci. (2021) 109575. doi:10.1016/j.corsci.2021.109575.

[12] A. Vinci, T. Reimer, L. Zoli, D. Sciti, Influence of pressure on the oxidation resistance of carbon fiber reinforced ZrB2/SiC composites at 2000 and 2200 °C, Corros. Sci. 184 (2021) 109377. doi:10.1016/j.corsci.2021.109377.

[13] D.M. Trucchi, A. Bellucci, M. Girolami, P. Calvani, E. Cappelli, S. Orlando, R. Polini, L. Silvestroni, D. Sciti, A. Kribus, Solar Thermionic-Thermoelectric

Generator (ST2G): Concept, Materials Engineering, and Prototype Demonstration, Adv. Energy Mater. 8 (2018) 1802310. doi:https://doi.org/10.1002/aenm.201802310.

[14] L. Zoli, S. Failla, E. Sani, D. Sciti, Novel ceramic fibre - Zirconium diboride composites for solar receivers in concentrating solar power systems, Compos. Part B Eng. 242 (2022) 110081. doi:10.1016/j.compositesb.2022.110081.

[15] F. Servadei, L. Zoli, P. Galizia, A. Vinci, D. Sciti, Development of UHTCMCs via water based ZrB_2 powder slurry infiltration and polymer infiltration and pyrolysis, J. Eur. Ceram. Soc. 40 (2020) 5076–5084. doi:10.1016/j.jeurceramsoc.2020.05.054.

[16] H. Hu, Q. Wang, Z. Chen, C. Zhang, Y. Zhang, J. Wang, Preparation and characterization of C/SiC-ZrB_2 composites by precursor infiltration and pyrolysis process, Ceram. Int. 36 (2010) 1011–1016. doi:10.1016/j.ceramint.2009.11.015.

[17] R. Liu, L. Yang, H. Miao, M. Jiang, Y. Wang, X. Liu, F. Wan, Influence of the SiC matrix introduction time on the microstructure and mechanical properties of Cf/Hf0.5Zr0.5C-SiC ultra-high temperature composites, Ceram. Int. 48 (2022) 3762–3770. doi:10.1016/J.CERAMINT.2021.10.159.

[18] Q. Li, S. Dong, Z. Wang, G. Shi, Fabrication and properties of 3-D Cf/ZrB2-ZrC-SiC composites via polymer infiltration and pyrolysis, Ceram. Int. 39 (2013) 5937–5941. doi:10.1016/j.ceramint.2012.11.074.

[19] Y. Blum, J. Marschall, H.J. Kleebe, Low temperature, low pressure fabrication of ultra high temperature ceramics (UHTCs), STAR. (2006). https://apps.dtic.mil/sti/citations/ADA456577.

[20] F. Uhlmann, C. Wilhelmi, S. Schmidt-Wimmer, S. Beyer, C. Badini, E.

Padovano, Preparation and characterization of ZrB_2 and TaC containing Cf/SiC composites via Polymer-Infiltration-Pyrolysis process, J. Eur. Ceram. Soc. 37 (2017) 1955–1960. doi:10.1016/j.jeurceramsoc.2016.12.048.

[21] M.S. Sarabjeet Kaur, Single-Source-Precursor Synthesis of SiC-Based Ceramic Nanocomposites for Energy-Related Applications Single-Source-Precursor Synthesis of SiC-Based Ceramic Nanocomposites for Energy-Related Applications, Technische Universität Darmstadt, 2016.

[22] S. Kaur, R. Riedel, E. Ionescu, Pressureless fabrication of dense monolithic SiC ceramics from a polycarbosilane, J. Eur. Ceram. Soc. 34 (2014) 3571–3578. doi:10.1016/j.jeurceramsoc.2014.05.002.

[23] Starfire® Systems Inc., StarPCS SMP-10, Technical Data Sheet, (2018).

[24] J. Yin, S.H. Lee, L. Feng, Y. Zhu, X. Liu, Z. Huang, S.Y. Kim, I.S. Han, The effects of SiC precursors on the microstructures and mechanical properties of SiCf/SiC composites prepared via polymer impregnation and pyrolysis process, Ceram. Int. 41 (2015) 4145–4153. doi:10.1016/j.ceramint.2014.11.112.

[25] B. Santhosh, E. Ionescu, F. Andreolli, M. Biesuz, A. Reitz, B. Albert, G.D. Sorarù, Effect of pyrolysis temperature on the microstructure and thermal conductivity of polymer-derived monolithic and porous SiC ceramics, J. Eur. Ceram. Soc. 41 (2021) 1151–1162. doi:10.1016/j.jeurceramsoc.2020.09.028.

[26] F*A*C*T - EQUILIB-Web, (n.d.).

[27] P. Colombo, G. Mera, R. Riedel, G.D. Sorarù, Polymer-derived ceramics: 40 Years of research and innovation in advanced ceramics, J. Am. Ceram. Soc. 93 (2010) 1805–1837. doi:10.1111/j.1551-2916.2010.03876.x.

[28] S.H. Lee, M. Weinmann, F. Aldinger, Particulate-Reinforced Precursor-Derived

Si–C–N Ceramics: Optimization of Pyrolysis Atmosphere and Schedules, J. Am. Ceram. Soc. 88 (2005) 3024–3031. doi:10.1111/J.1551-2916.2005.00587.X.

[29] S. Kimura, E. Yasuda, H. Tanaka, S. Yamada, Graphitization and microstructure of carbon fiber/glassy carbon composite, Yogyo-Kyokai-Shi. 83 (1975) 122–127.

[30] S. Kimura, FRACTURE BEHAVIOUR OF CARBON-FIBER/CVD CARBON COMPOSITES, (1981).

[31] S. Kimura, Y. Tanabe, N. Takase, E. Yasuda, PRESSURE GRAPHITIZATION OF MATRIX IN CARBON-FIBER GLASS-LIKE CARBON COMPOSITE, Nippon Kagaku Kaishi. (1981) 1474–1480.

[32] Y. Seyrek, K.T. Felekoğlu, Selection of proper matrix with plasma-treated HTPP fiber reinforced cementitious composites in terms of flexural toughness, J. Build. Eng. 45 (2022) 103632. doi:10.1016/J.JOBE.2021.103632.

[33] A. Saha, R. Raj, Crystallization Maps for SiCO Amorphous Ceramics, J. Am. Ceram. Soc. 90 (2007) 578–583. doi:10.1111/J.1551-2916.2006.01423.X.

Supplementary material

Effect of annealing treatments on the mechanical behaviour of UHTCMCs prepared by Mild Polymer Infiltration and Pyrolysis

Francesca Servadei, Luca Zoli*, Pietro Galizia, Cesare Melandri, Simone Failla, Diletta Sciti

CNR-ISTEC, Institute of Science and Technology for Ceramics, Via Granarolo 64, I-48018 Faenza, Italy

**Author to whom correspondence should be addressed: Luca Zoli, luca.zoli@istec.cnr.it*

Table S1. Bulk density (via geometric and Archimedes' method), skeletal density, open porosity, weight loss and volume variations of reference sample 6PIP-10 and annealed samples at 1100–1900°C.

Sample	Annealing cycle (°C)	Bulk $d_{geom.}$ (g/cm^3)	Bulk $d_{Arch.}$ (g/cm^3) *	Skeletal d (g/cm^3) *	Open poros. (%) *	wt. loss (%)	ΔV (%)
6PIP-10	-	3.01 ± 0.06	3.17	3.36	5.7	-	-
A-11	1100	3.01 ± 0.01	3.13	3.39	7.8	-0.41 ± 0.03	0.0
A-12	1200	2.99 ± 0.01	3.15	3.36	6.3	-0.60 ± 0.09	0.0
A-13	1300	3.00 ± 0.06	3.15	3.40	8.0	-0.71 ± 0.02	0.0
A-14	1400	2.97 ± 0.03	3.13	3.41	8.2	-2.28 ± 0.58	0.5 ± 0.2
A-15	1500	2.72 ± 0.10	2.78	3.45	19.3	-6.47 ± 1.67	1.9 ± 0.7
A-16	1600	2.59 ± 0.04	2.62	3.77	30.5	-9.75 ± 0.18	4.5 ± 0.4
A-17	1700	2.58 ± 0.07	2.68	3.87	30.7	-9.73 ± 0.15	6.1 ± 1.4
A-18	1800	2.54 ± 0.02	2.66	3.87	31.2	-9.75 ± 0.14	7.3 ± 2.9
A-19	1900	2.44 ± 0.25	2.60	3.94	31.5	-10.04 ± 0.18	11.2 ± 10.8

* measurement by Mercury Intrusion Porosimetry (MIP)

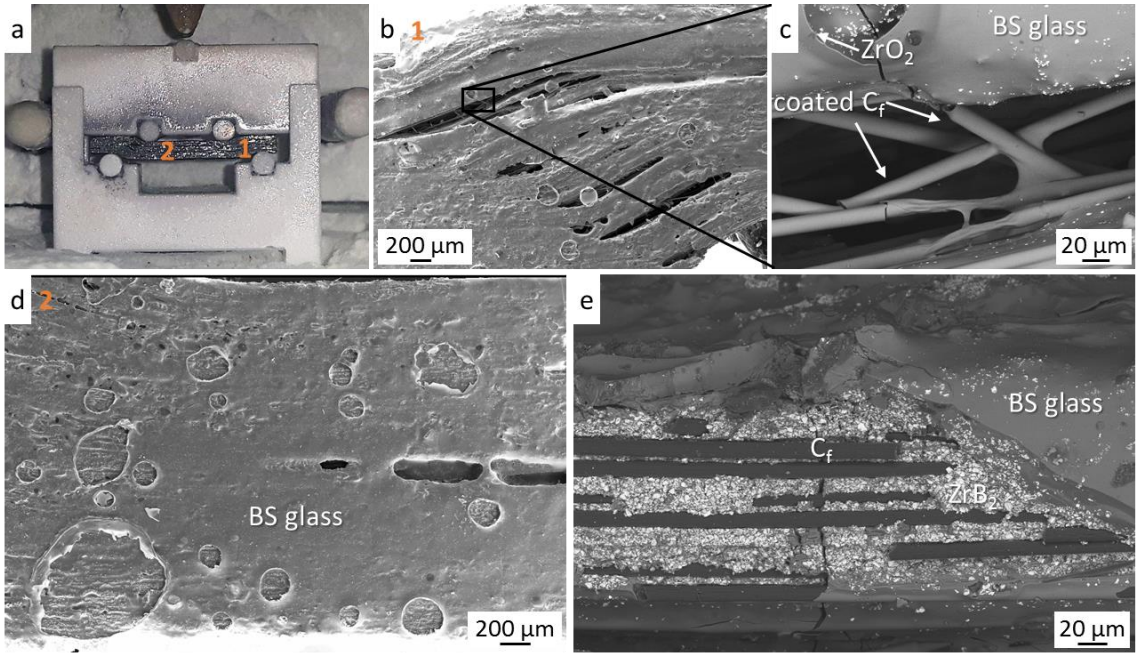

Fig. S1. (a) Optical image of bar of sample 6PIP-10 tested by bending test at 1500°C under Ar flow, deformed plastically on alumina fixture. (b) SEM image (lateral view) in deformed point under load pin (indicated as 1 in (a)) highlighting opening among layers and (c) magnification of carbon fibres coated by borosilicate glass. (d) SEM image (lateral view) in the middle part (indicated as 2 in (a)). (e) SEM image (BSE signal) of undamaged fibres underneath BS glass.

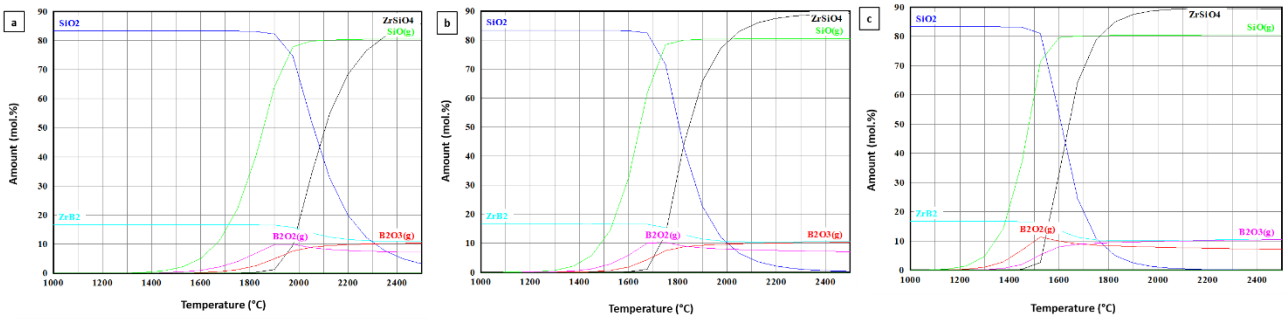

Fig. S2. Isobaric multiphase equilibria as function of the temperature calculated using HSC Chemistry v.6.1 for the ZrB_2-SiO2 system at the pressure of : a) 1 bar, b) 0.1 bar, 0.01 bar.

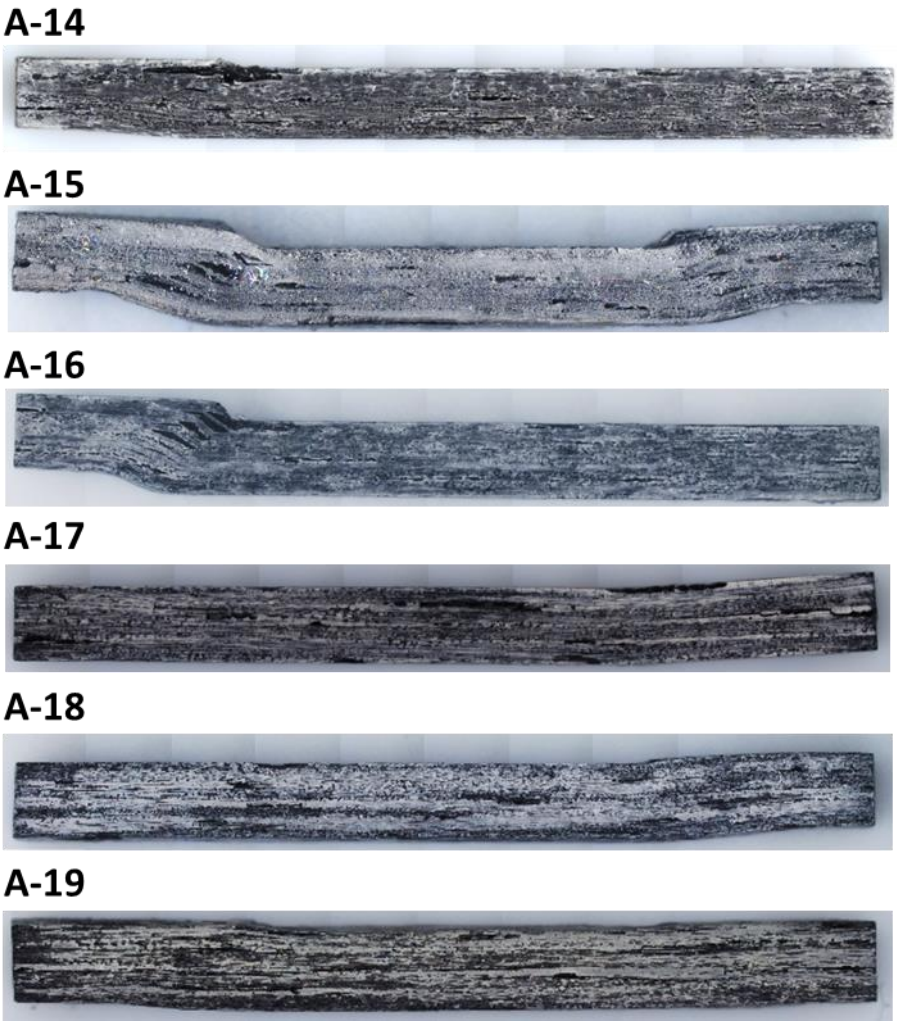

Fig. S3. Optical images (lateral view) of bars annealed at 1400-1900°C and tested by 4-pt bending test at 1500°C under Ar flow.

Declaration of interests

☒ The authors declare that they have no known competing financial interests or personal relationships that could have appeared to influence the work reported in this paper.

☐The authors declare the following financial interests/personal relationships which may be considered as potential competing interests: